

## **Supporting information**

### **Self-supported beaded Au@Co<sub>3</sub>O<sub>4</sub> nanowire arrays electrocatalytic CO<sub>2</sub> in water to syngas and water oxidation to O<sub>2</sub>**

Shi-Yuan Zhang, Jing-Jing Ma, Hong-Lin Zhu, Yue-Qing Zheng\*

Chemistry Institute for Synthesis and Green Application, Ningbo University, Ningbo, 315211, P.  
R. China

\*Corresponding author: Yue-Qing Zheng

E-mail address: zhengyueqing@nbu.edu.cn

Tel/fax: +86 574 87600747

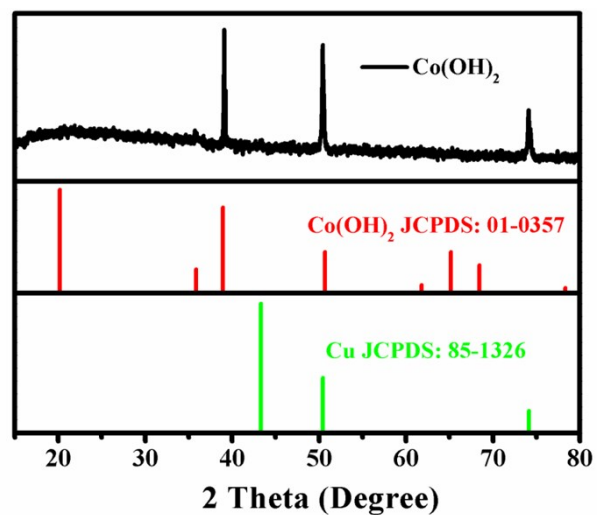


Figure S1 PXRD pattern of Co(OH)<sub>2</sub> NAs on Cu foam.

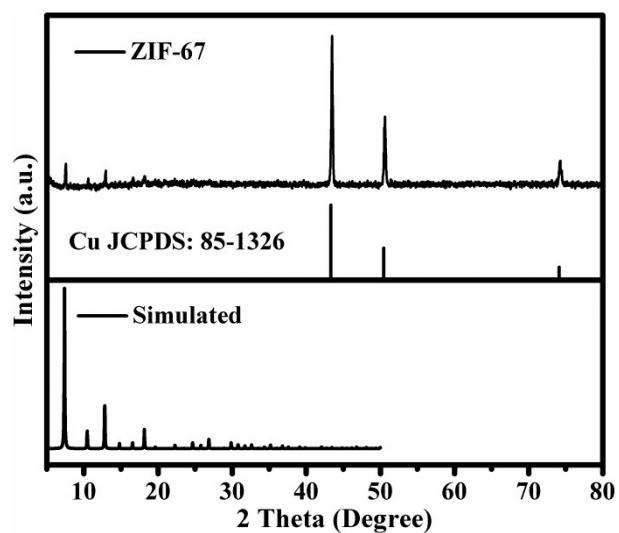


Figure S2 PXRD pattern of beaded ZIF-67 NAs on Cu foam.

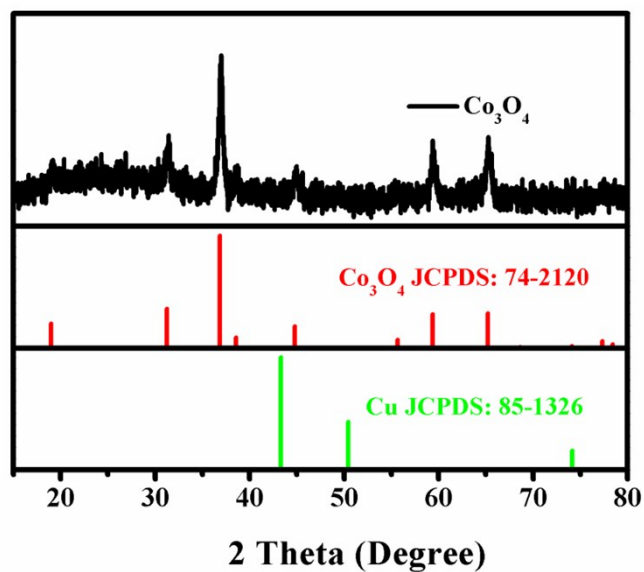
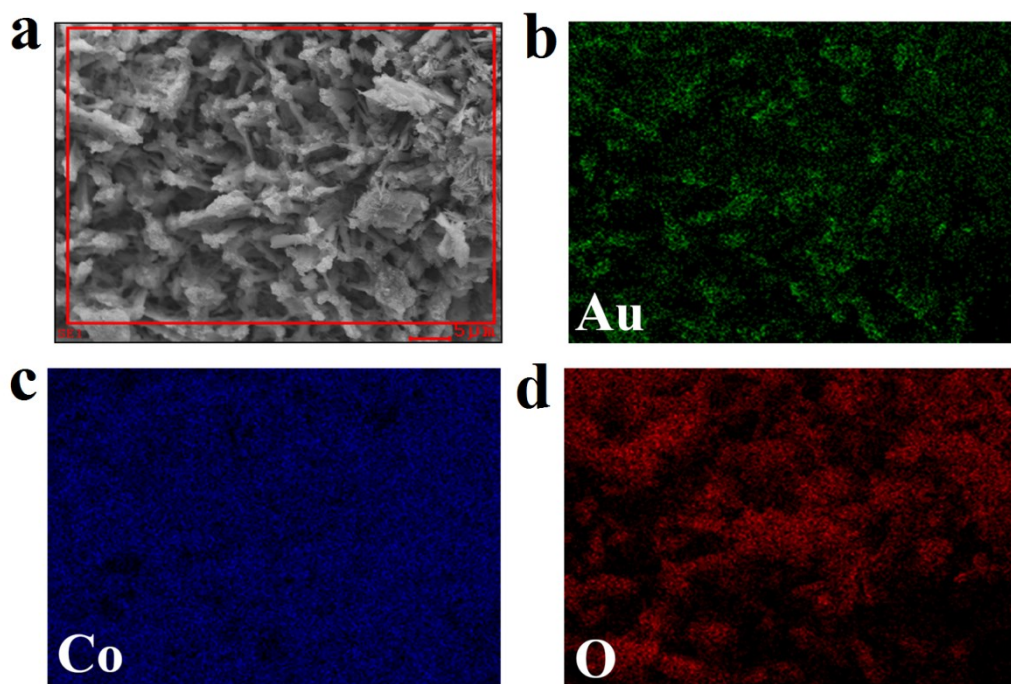
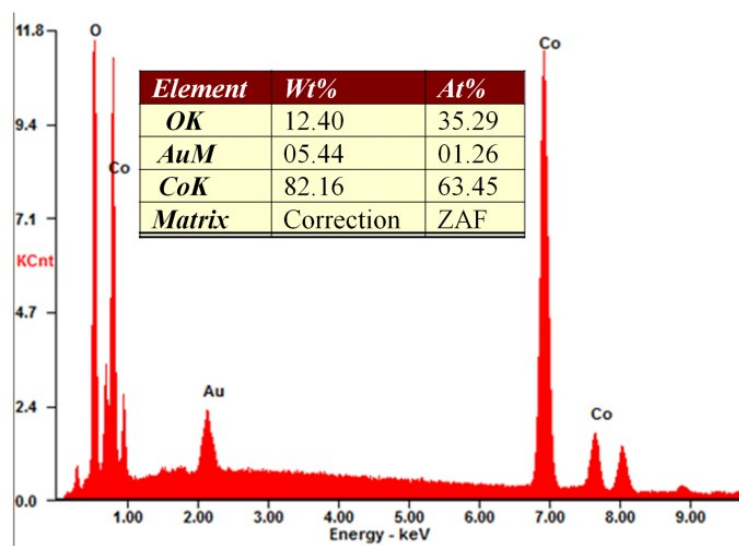


Figure S3 PXRD pattern of beaded Co<sub>3</sub>O<sub>4</sub> NAs on Cu foam.



**Fig.S4** (a) SEM images of Au@Co<sub>3</sub>O<sub>4</sub> NAs on Cu foam after electrolysis and corresponding elemental mapping images of Au (b), Co (c) and O (d).



**Figure S5** EDX spectrum of Au@Co<sub>3</sub>O<sub>4</sub> NAs on Cu foam after electrolysis.

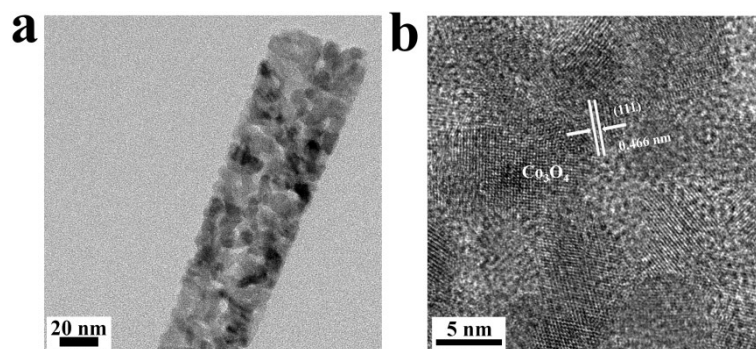


**Figure S6** TEM and HRTEM images of  $\text{Co}_3\text{O}_4$  NAs.

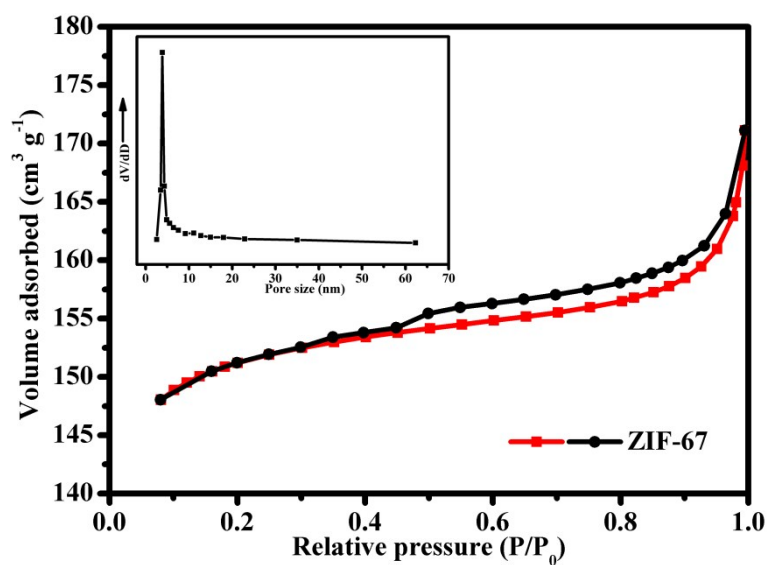


**Figure S7**  $\text{N}_2$  adsorption-desorption isotherm and the pore size distribution of the ZIF-67 NAs.

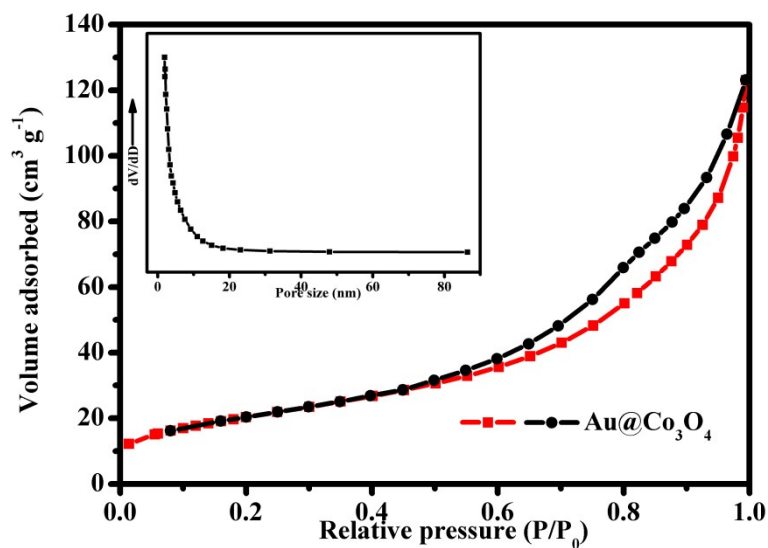


**Figure S8**  $\text{N}_2$  adsorption-desorption isotherm and the pore size distribution of the  $\text{Au}@\text{Co}_3\text{O}_4$  NAs.

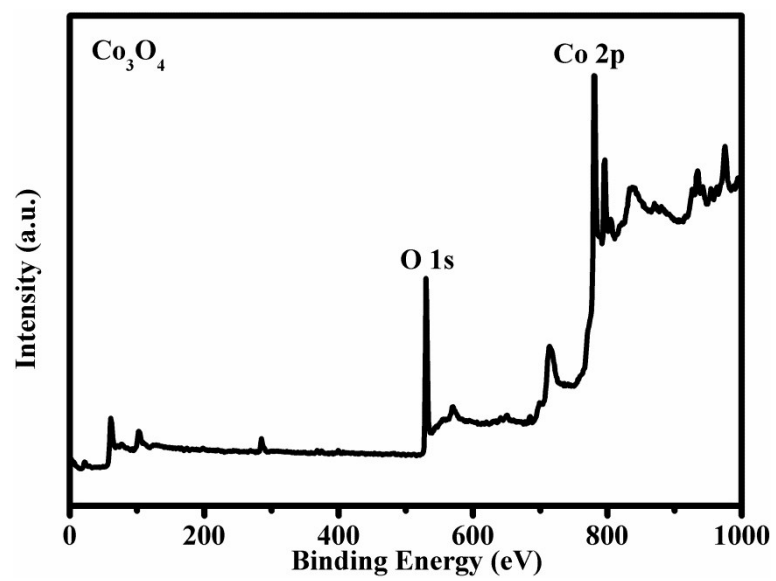


**Figure S9** XPS survey spectrum of  $\text{Co}_3\text{O}_4$  material.

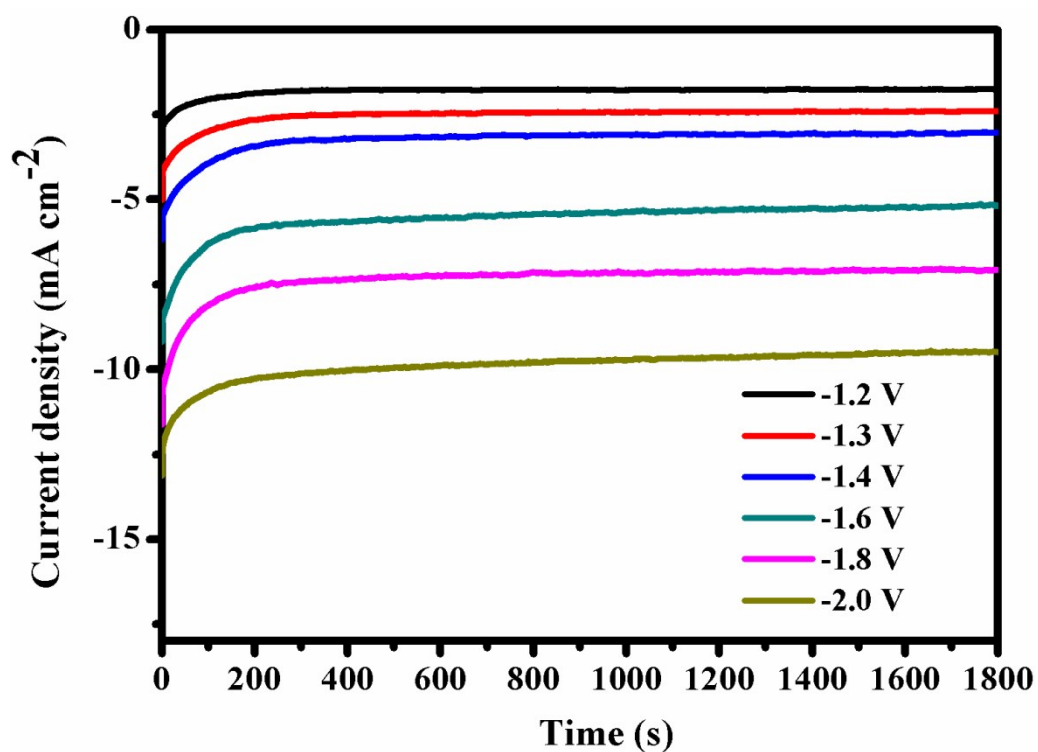


**Figure S10** CPE plots for Cu foam in 0.1 M KHCO<sub>3</sub> at different potentials under CO<sub>2</sub> during 1800 s, respectively.

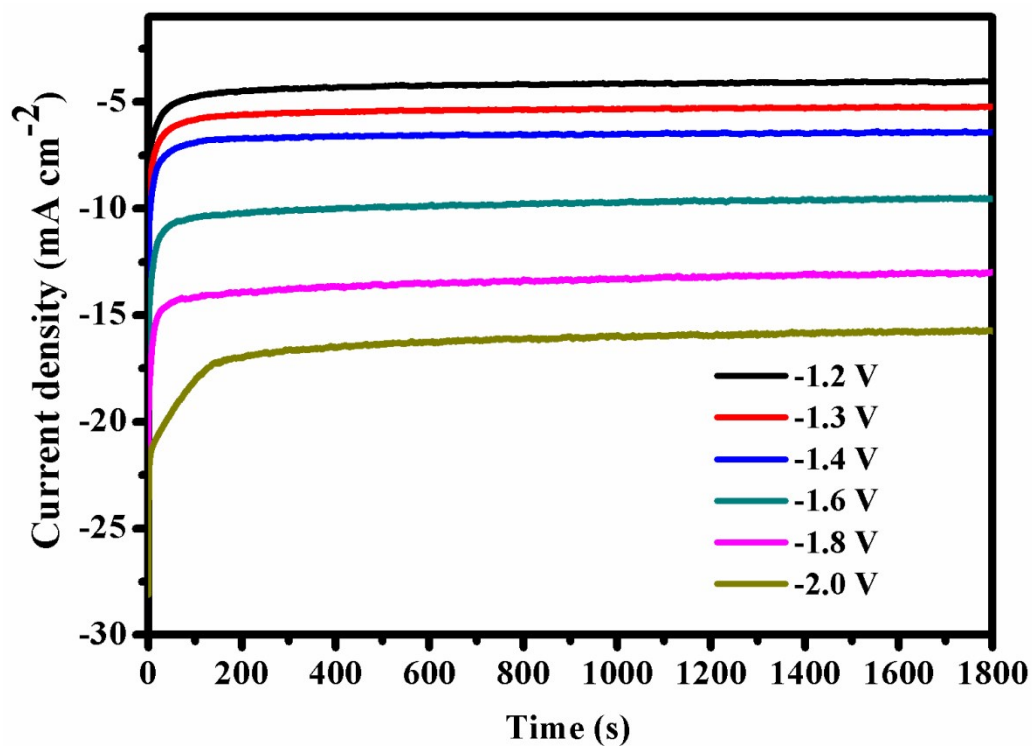


**Figure S11** CPE plots for Co<sub>3</sub>O<sub>4</sub> NAs in 0.1 M KHCO<sub>3</sub> at different potentials under CO<sub>2</sub> during 1800 s, respectively.

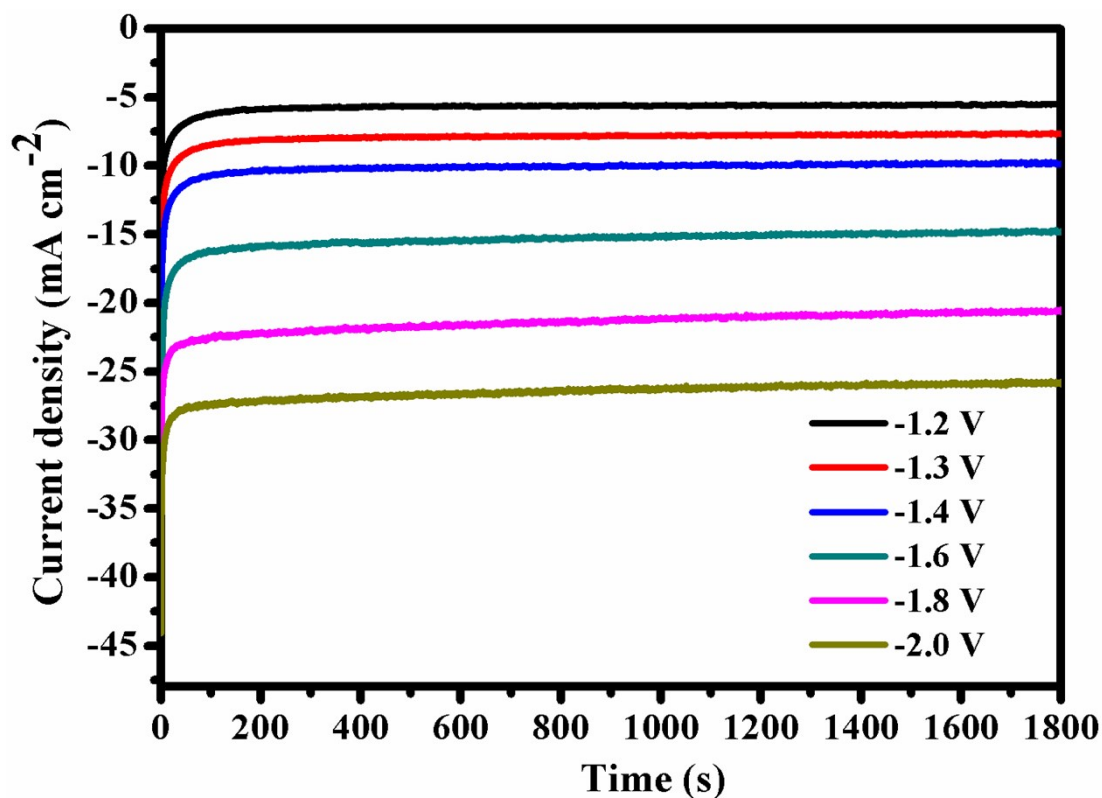


**Figure S12** CPE plots for Au@Co<sub>3</sub>O<sub>4</sub> NAs in 0.1 M KHCO<sub>3</sub> at different potentials under CO<sub>2</sub> during 1800 s, respectively.

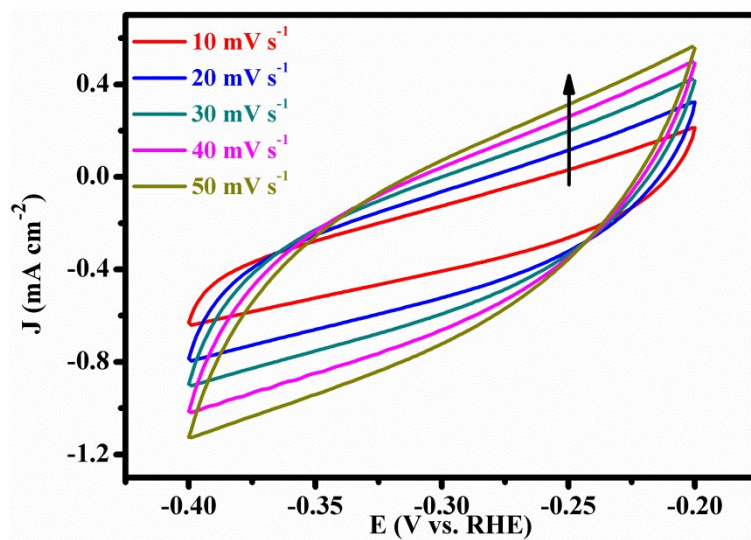


**Figure S13** CVs of Co<sub>3</sub>O<sub>4</sub> NAs recorded at different scan rates (10, 20, 30, 40 and 50  $\text{mV s}^{-1}$ ).



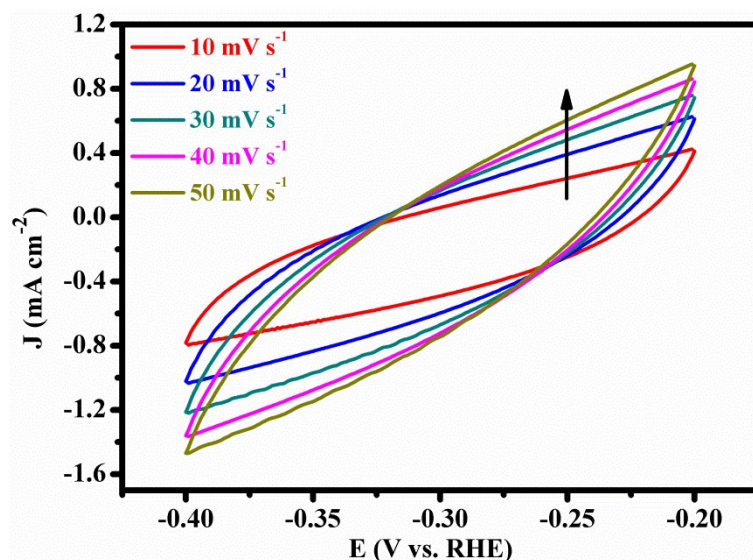


**Figure S14** CVs of Au@Co<sub>3</sub>O<sub>4</sub> NAs recorded at different scan rates (10, 20, 30, 40 and 50 mV s<sup>-1</sup>).

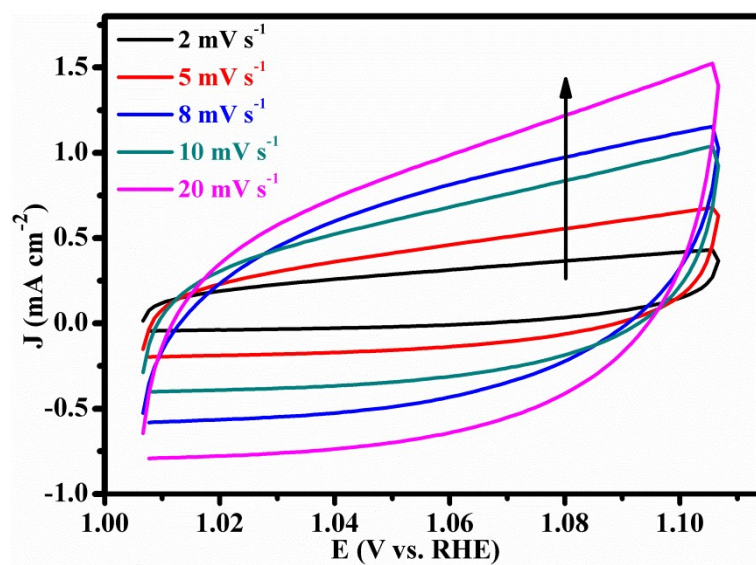


**Figure S15** CVs of Co<sub>3</sub>O<sub>4</sub> NAs recorded at different scan rates (2, 5, 8, 10 and 20 mV s<sup>-1</sup>).



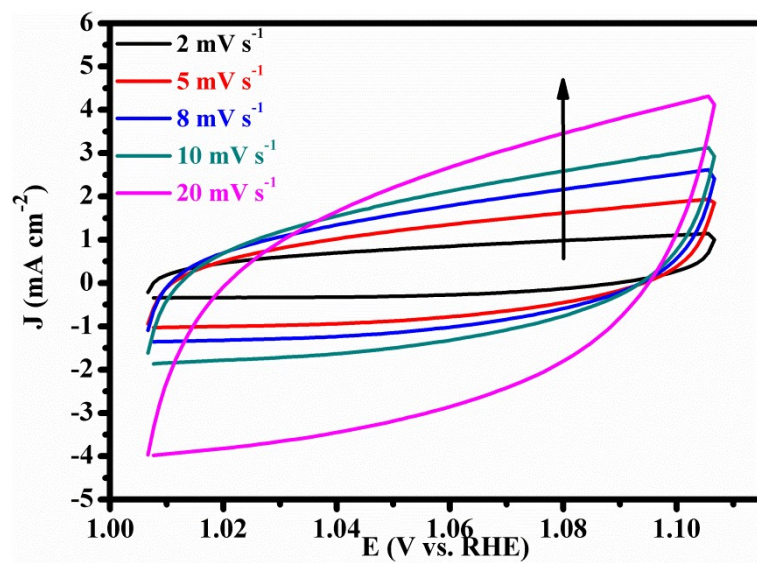


**Figure S16** CVs of Au@Co<sub>3</sub>O<sub>4</sub> NAs recorded at different scan rates (2, 5, 8, 10 and 20 mV s<sup>-1</sup>).

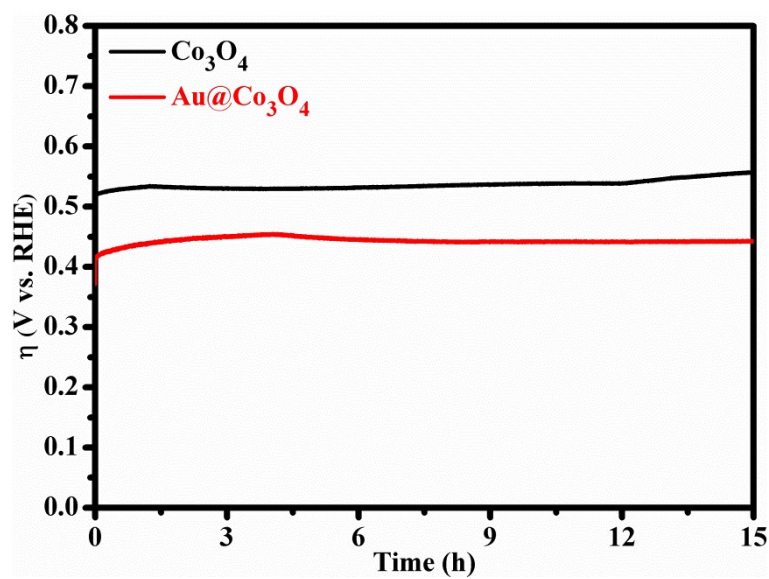


**Figure S17** CP plots for  $\text{Au@Co}_3\text{O}_4$  NAs and  $\text{Co}_3\text{O}_4$  NAs in 1.0 M KOH at  $50 \text{ mA cm}^{-2}$ .

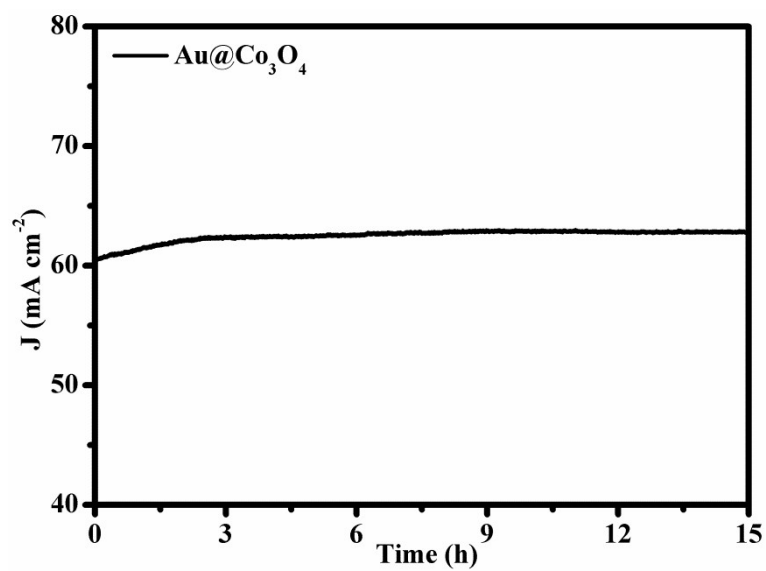


**Figure S18** CPE plot for  $\text{Au@Co}_3\text{O}_4$  NAs in 1.0 M KOH at 1.7 V vs. RHE.

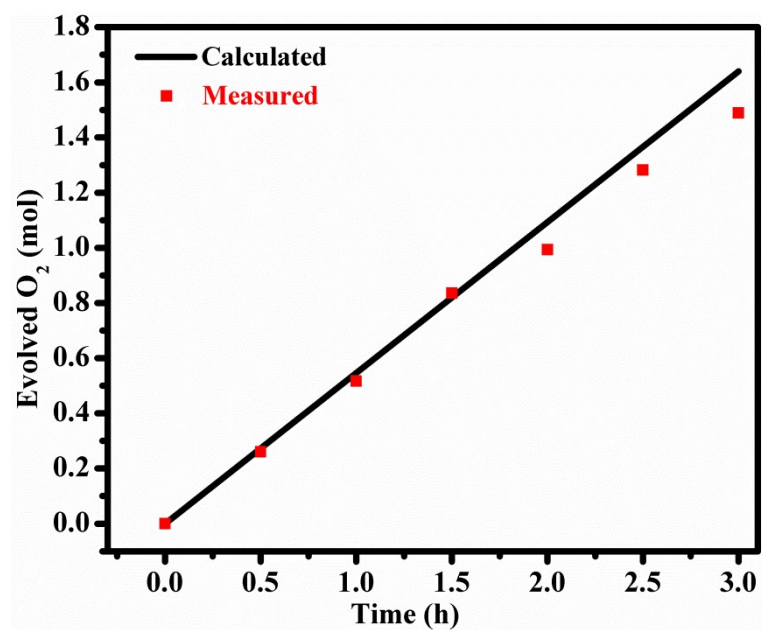


**Figure S19** Calculated and measured oxygen amount against electrolysis time for Au@Co<sub>3</sub>O<sub>4</sub> NAs at the fixed potential of 1.70 V vs. RHE.

---